UNIVERSITY OF CALIFORNIA
SANTA CRUZ

A REVIEW OF PROPULSIVE DESCENT FUEL OPTIMIZATION GUIDANCE METHODS FOR PLANETARY PINPOINT LANDINGS

A thesis submitted in partial satisfaction of the
requirements for the degree of

BACHELOR OF SCIENCE

in

PHYSICS

by

Kent L. Roberts

June 2019

The Thesis of Kent L. Roberts
is approved:

_____
Professor Robert Johnson, Chair

_____
Professor Qi Gong

_____
Professor Terry Terhaar

Abstract

A Review of Propulsive Descent Fuel Optimization Guidance Methods for Planetary Pinpoint Landings

by

Kent L. Roberts

In this paper, the APDG (Apollo Powered Descent Guidance), A^{2}PDG (Augmented Apollo Powered Descent Guidance), and SOCP (Second-Order Cone Programming) powered descent guidance methods are explored and compared. While fuel optimization is the focus of any solution to the soft-landing problem, it is clear that the aforementioned guidance techniques adopt fundamentally different approaches. APDG is one of the most straightforward and simplistic techniques examined. A^{2}PDG builds upon the heritage of the APDG method to introduce a tunable implicit guidance law that enables a trade between trajectory shaping and propellant consumption. The SOCP method examined represents a modern approach leveraging the forefront of optimal control theory research into SOCP problems and the interior point methods (IPMs) used to solve them. The SOCP technique achieves both landing-error and fuel optimization, while respecting nearly all constraints and boundary conditions representative of the physical problem. By identifying the strengths and weaknesses of available powered descent guidance methods, goals can be set to derive new techniques and the best-fit guidance scheme can be matched to the demands of future space exploration missions.

Table of Contents

List of Figures

List of Tables

Chapter 1

Introduction

This year (2019) will mark the fiftieth anniversary of the Apollo lunar landing and the seventh operational year of NASA's *Curiosity* rover on the surface of Mars. While the destinations, goals, and technologies of these two missions differ greatly, both relied on powered descent guidance to accomplish their objectives. Powered descent is the final phase of many entry, descent and landing (EDL) architectures, during which a payload is guided and softly landed on a planet's or moon's surface. This is accomplished by firing rocket engines retro-propulsively (counter to a spacecraft's motion) to decelerate the vehicle and guide it towards a destination. While not all extra-terrestrial surface exploration missions include a terminal powered descent, the prevalence of the maneuver is increasing as planetary exploration missions grow in mass and narrow in focus.

The *Curiosity* rover represents the mass limit of modern Mars EDL capabilities at approximately 1 metric ton; estimates for a human mission to Mars demand between 40-80

metric tons of landed mass (Braun and Manning, 2007). Mars has an atmosphere capable of partially decelerating a spacecraft from orbital velocities; however, as the mass of entry vehicles increase, the deceleration available via atmospheric drag diminishes. This follows since drag is proportional to a vehicle's cross-sectional area that typically scales at a rate sub-linearly with its mass. Therefore as missions increase in mass, the powered descent phase will account for a larger portion of a vehicle's total deceleration. Refinement of powered descent guidance techniques will directly benefit these future missions.

Fuel optimization during a powered descent is critically important to a planetary exploration mission's feasibility and ultimate success. Fuel optimal trajectories require less propellant to be transported from an initial Earth launch to a mission's target. This allows a greater fraction of the mission's overall mass budget to be dedicated to scientific instrumentation. Alternatively, for a set amount of propellant, fuel optimal trajectories expand the envelope of correction maneuvers available to avoid hazards and adapt to initial state errors or uncertainties.

Historically, the first generation of Mars surface missions (Viking, Mars Pathfinder, and the Mars Exploration Rovers) were exploration driven. The nature of these missions were forgiving of large landing ellipses (a measure of landing location uncertainty) on the order of 100 km (Brand et al., 2004). In contrast, modern Mars exploration programs have evolved to pursue focused scientific goals, targeting specific surface features such as craters or potential regions of sub-surface water ice. Improvements in powered descent guidance directly contributes towards providing the landing precision that modern missions demand.

The powered descent guidance problem (also referred to as the soft-landing problem) involves designing a fuel-optimized thrust profile that transports a vehicle from initial conditions

to soft-landing conditions on a planet's or other celestial body's surface. Broadly speaking, the powered descent guidance problem is classified as a finite-horizon optimal control problem and while a closed-form analytical solutions exist in the one-dimensional case it does not remain optimal when extended to the full three-dimensional case if proper state and control constraints are applied (Akmee et al., 2013). A number of solution methods have been developed, two of which, the Augmented Apollo Powered Descent Guidance (A^2PDG) and Second-Order Cone Programming (SOCP) techniques serve as the primary focus of this study. A^2PDG builds upon the heritage of the APDG method to introduce a tunable implicit guidance law enabling a trade between trajectory shaping and propellant consumption, while the SOCP method represents a modern approach leveraging the forefront of optimal control theory.

Chapter 2 will present a one-dimensional formulation of the problem, summarizing the landmark optimization work of Meditch (1964) and demonstrating a simplified Apollo based guidance algorithm, while Chapters 3 and 4 will discuss the A^2PDG and SOCP solution methods respectively. Chapter 5 will compare all methods discussed, with conclusions being presented in Chapter 6.

Chapter 2

The 1D Powered Descent Guidance Problem

Consider a spacecraft attempting to land on a flat planetary surface surrounded by vacuum (Figure 2.1) and assume the following: 1) the vehicle only experiences the forces of gravitational attraction to the surface and the thrust it generates, 2) the thrust vector is constrained normal to the surface, 3) gravity does not vary with altitude, 4) the thrust (and hence propellant flow rate) is limited between zero and a set maximum, and 5) that the vehicle has sufficient fuel to perform a propulsive landing.

Given this, the vehicle's motion will be governed by the following equation:

$$\ddot{x} = \frac{-v_e \dot{m}}{m} - g. \tag{2.1}$$

where x represents the altitude of the vehicle, v_e denotes the effective exhaust velocity and is

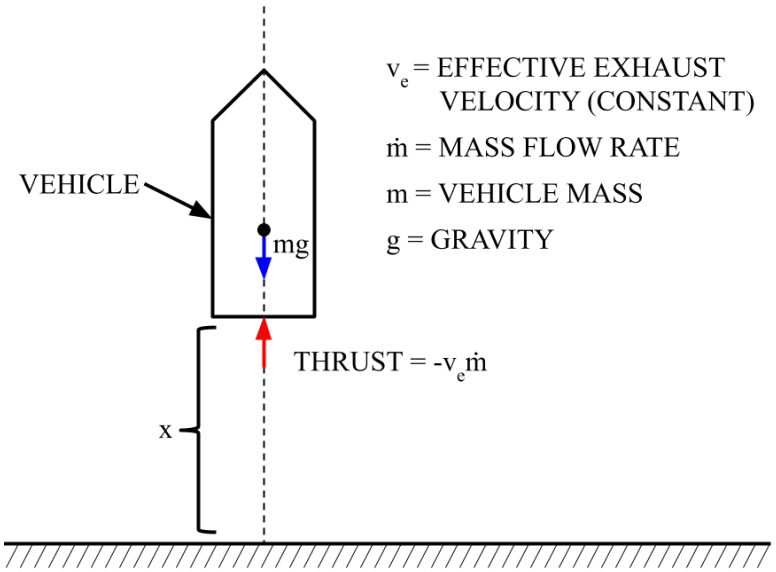

Figure 2.1: Schematic of the 1D soft-landing problem

always positive ($v_e \geq 0$). The mass of the vehicle is represented by m, while $\dot{m}$ denotes the mass flow rate and is bounded by extrema α and 0 ($-\alpha \leq \dot{m} \leq 0$).

The one-dimensional powered descent guidance problem is thus framed as the following system of equations:

$$\dot{x_1} = x_2; \qquad \dot{x_2} = -\frac{v_e}{x_3}u - g; \qquad \dot{x_3} = u \tag{2.2}$$

with

$$x_1 = x; \qquad x_2 = v_x; \qquad x_3 = m. \tag{2.3}$$

The variable u represents the control parameter $\dot{m}$, or equivalently the magnitude of the commanded thrust T_c (note that the two differ only by a constant factor of v_e).

The total fuel consumption is calculated via the following equation, and also represents the cost function to be minimized:

$$J = \int_0^{t_f} \dot{m}(t)dt = m(0) - m(t_f). \tag{2.4}$$

Where some final time t_f is left unconstrained. The variable t_f is also used to define the terminal boundary conditions of a soft-landing:

$$x(t_f) = 0; \qquad \dot{x}(t_f) = 0. \tag{2.5}$$

Together, equations 2.2, 2.4, and 2.5 define the basic form of the one-dimensional soft-landing problem.

2.1 Meditch's Switching Function

Meditch (1964) serves as a baseline and historic reference for soft-landing guidance research. Published near the onset of the Apollo program, Meditch analytically optimized the one-dimensional powered descent guidance problem.

The method includes first combining of equations 2.1 and 2.4 yeilding:

$$J = m(0)\left(1 - \exp\left[\frac{\dot{x}(0) - gt_f}{v_e}\right]\right). \tag{2.6}$$

And next, true insight is gained by recognizing that for a given $m(0)$, $\dot{x}(0)$, g, and v_e, J is a monotonically increasing function of t_f and thus, minimizing t_f is equivalent to minimizing fuel consumption (Meditch, 1964).

Using the Pontryagin maximum principle to optimize the system, It is found that the optimal control equation takes the form of a step function (Meditch, 1964). Physically, this translates to a period of free fall with no control input, abruptly followed by a period of maximum thrust and deceleration.

The switching point is determined when the following function changes from a positive value to 0 (Meditch, 1964):

$$f(x_1, x_2) = \frac{b}{a} x_1 + 2a\sqrt{\frac{x_1}{a}} + x_2 \tag{2.7}$$

with the a and b parameters defined as:

$$a = \frac{1}{2}\left(\frac{v_e(-\dot{m}) - gM_0}{M_0}\right) \tag{2.8}$$

$$b = \frac{v_e(\dot{m})^2}{2M_0^2}. \tag{2.9}$$

Thus, the fuel optimal one-dimensional soft-landing guidance scheme is proven to be a switch from 0 to full thrust, governed by equation 2.7.

2.2 Apollo Guidance in 1D

As flown, the Apollo powered descent guidance scheme assumed the magnitude of each component of the thrust acceleration vector to be a quadratic function of time (Klumpp, 1974). Thus for each of the component directions the acceleration profile would take the form of:

$$a(t) = C_0 + C_1 t + C_2 t^2. \tag{2.10}$$

Integrating equation 2.10 to determine the velocity and altitude profiles as functions of time, while observing the initial and final conditions yields analytic solutions for the C_0, C_1, and C_2 constants (Steinfeldt et al., 2008):

$$C_0 = a_f - \frac{6}{t_{go}}(v_f + v_0) + 12(x_f - x_0) \tag{2.11}$$

$$C_1 = -\frac{6}{t_{go}}a_f + \frac{6}{t_{go}^2}(5v_f + 3v_0) - \frac{48}{t_{go}^3}(x_f - x_0) \tag{2.12}$$

$$C_2 = \frac{6}{t_{go}^2}a_f - \frac{12}{t_{go}^3}(2v_f + v_0) + \frac{36}{t_{go}^4}(x_f - x_0), \tag{2.13}$$

where t_{go} represents the travel time left between the current and final states. The value of t_{go} can be solved analytically if the acceleration profile is further simplified to a linear function of time ($C_2 = 0$). This linear approach is widely referred to as E-guidance as is identical to the one-dimensional adaptation of the APDG law if a_f is set to be 0. This is a reasonable requirement in the applications of guidance laws since powered descent maneuvers typically include a final constant-velocity touch down phase just before surface contact. The difference between these two methods (E-guidance and APDG) is more apparent in three-dimensions where the APDG law's quadratic acceleration profile requires a final acceleration state vector to be specified $\mathbf{a}_T(t_f)$, which includes both a magnitude and direction.

Returning to the one-dimensional case, t_{go} can be solved for as follows (Wong et al., 2002):

$$t_{go} = \frac{2v_f + v_0}{a_f} + \left[\left(\frac{2v_f + v_0}{a_f} \right)^2 + \frac{6}{a_f}(x_0 - x_f) \right]^{1/2}, \qquad a_f \neq 0 \tag{2.14}$$

$$t_{go} = 3\frac{r_f - r_0}{2v_f + v_0}, \qquad a_f = 0. \tag{2.15}$$

Given that $a_f = 0$ and setting the soft-landing conditions $v_f = 0$ and $x_f = 0$, equations 2.10, 2.11, 2.12, and 2.15 can be combined to determine an acceleration profile:

$$a(t) = \frac{2}{3}\frac{v_0^2}{x_0} + \frac{2}{9}\frac{v_0^3}{x_0^2}t. \tag{2.16}$$

This profile is constantly updated with the state of system defined by the current altitude x_0 and altitude rate v_0. It is important to note that in the vicinity of the surface $t_{go} \to 0$ and in this limit, the coefficients C_1 and C_2 become singularities. The work-around is to record the last time the C_i constants were calculated (denoted as t_C) and use the formula (Wong et al., 2002):

$$a(t) = C_0 + C_1(t - t_C) + C_2(t - t_C)^2. \tag{2.17}$$

Therefore, an acceleration profile can be calculated at any state, and a commanded thrust (T_c) can be derived by substituting the derived acceleration into the dynamic equation:

$$T_c = m(a - g) \tag{2.18}$$

Thus the APDG method is defined as an explicit guidance law (capable of calculating a full trajectory profile based on only the state of the system) with the assumption that the acceleration profile is a quadratic function of time.

2.3 Numerical 1D Demonstration

To provide more insight into the operation of the one-dimensional formulations of the APDG and Meditch methods, both are applied to an example lunar descent scenario described in Table 2.1. The dynamics of the system is simulated using a discretized forward Euler integration method.

	Symbol	Value
Local Surface Gravity	g	-1.62 m/s^2
Effective Exhaust Velocity	v_e	3050 m/s
Initial Vehicle Mass	M_0	6000 kg
Maximum Thrust	T_{max}	45 kN
Initial Altitude	x_i	500 m
Initial Altitude Rate	v_i	-30 m/s
Final Altitude Target	x_f	0 m
Final Altitude Rate Target	v_f	0 m/s

Table 2.1: Vehicle and initial state parameters used in the example 1D lunar descent simulation

Figure 2.2 depicts the thrust control profiles results from a one-dimensional application of the Meditch and Apollo methods to the example lunar descent scenario. Notably during the initial phase of the APDG descent, the commanded thrust approaches 0. While the descent propulsion system of the Apollo lander was designed to be deeply throttle-able (down to 10% of maximum thrust) the guidance law still issues infeasible commands. A similar control saturation is apparent during the final approach phase resulting in a plateau of maximum thrust.

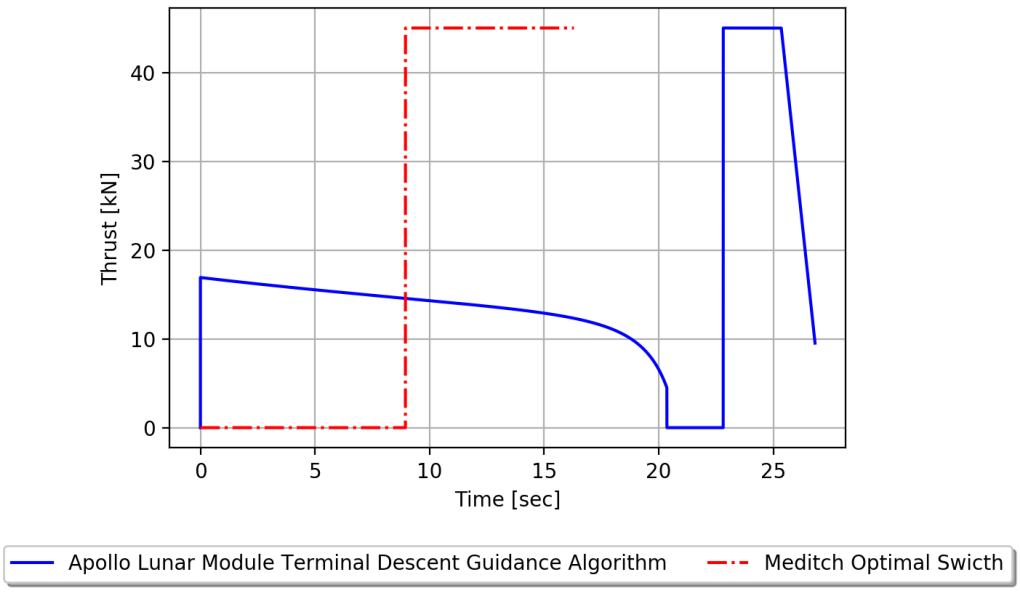

Figure 2.2: Thrust control profiles of the one-dimensional fuel optimal Meditch switch function (in red) and the Apollo guidance algorithm (in blue) applied to the example lunar descent scenario

Figure 2.3 depicts the descent rates of these two methods plotted against altitude. Note that the simulated APDG trajectory shape is in good agreement with the reference, Figure 19 of Bennett (1970). Figure 2.3 also graphically represents the risk of practically implementing an optimal switching technique. A slight error in powered descent initiation (PDI) can lead to irreversible crashing descent scenarios. In figure 2.3, the sharp corners of each trajectory (at $\sim$170m for the Meditch method and $\sim$40m for the APDG method) indicate the last possible opportunities to abort the descent.

Ultimately, the simulation shows that the optimal Meditch switching trajectory consumed 33% less propellant than the Apollo guidance path. However, this comparison highlights

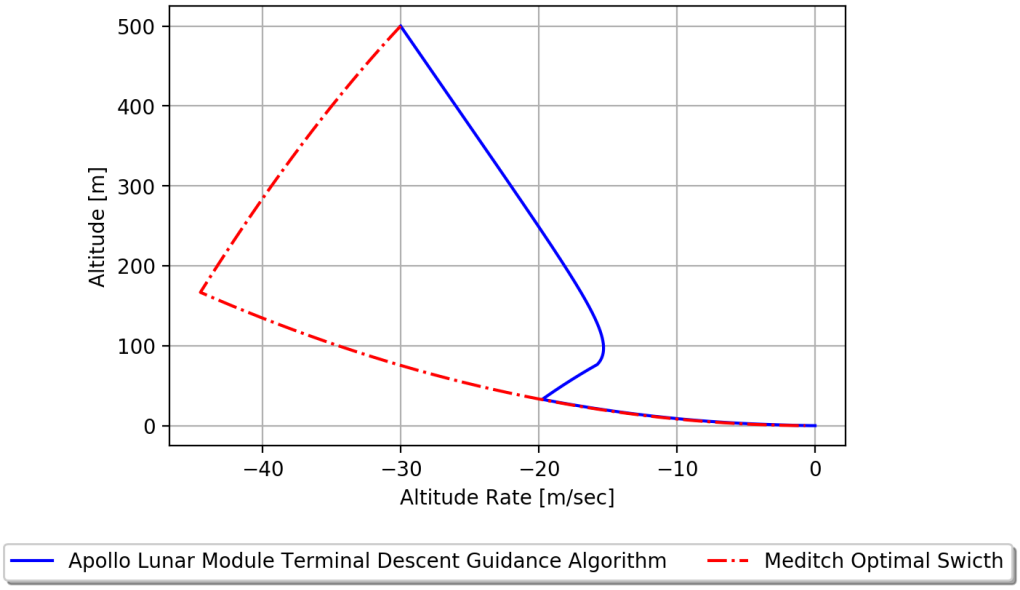

Figure 2.3: A plot of the descent rate versus altitude profiles of the one-dimensional fuel optimal Meditch switch function (in red) and the Apollo guidance algorithm (in blue) applied to the example lunar descent scenario. Note that the Apollo trajectory shape is in good agreement with figure 19 of Bennett (1970).

the fact that fuel consumption does not overshadow all factor considered in the selection of a guidance method. APDG was developed to maximize the allowable abort time to safeguard the astronauts on-board (Bennett, 1970).

Chapter 3

Augmented Apollo Powered Descent Guidance (A^2PDG)

The soft-landing problem in three dimensions can be stated as follows: given the system dynamics,

$$\dot{\mathbf{x}} = \mathbf{v}; \qquad \dot{\mathbf{v}} = \mathbf{g} + \mathbf{a_T} \tag{3.1}$$

and current measurable state values, $\mathbf{x}(t)$ and $\mathbf{v}(t)$, solve for the thrust command $\mathbf{a_T}(t)$ to maneuver the vehicle to a final state, $\mathbf{x}_f$ and $\mathbf{v}_f$ (Note that these quantities are now represented as vectors).

In a similar fashion to equation 2.10, the derivation of the A^2PDG law begins with the assumption that acceleration is a quadratic function of time in each component direction:

$$\mathbf{a}(t) = \mathbf{C_0} + \mathbf{C_1}t + \mathbf{C_2}t^2 \tag{3.2}$$

By specifying a boundary acceleration constraint $\mathbf{a_f}$, the 3D APDG law follows:

$$\mathbf{a}(t) = -\frac{6}{t_{go}}[\mathbf{v_f} - \mathbf{v}(t)] + \frac{12}{t_{go}^2}[\mathbf{x}_f - \mathbf{x}(t) - \mathbf{v}(t)t_{go}] + \mathbf{a}_f. \tag{3.3}$$

This formula is modified and relaxed, adopting the form of an implicit guidance law and defining the A^{2}PDG method (Lu, 2018):

$$\mathbf{a}(t) = \mathbf{a}_d(t) - \frac{k_v}{t_{go}}[\mathbf{v}(t) - \mathbf{v}_d(t)] - \frac{k_r}{t_{go}^2}[\mathbf{x}(t) - \mathbf{x}_d(t)] \tag{3.4}$$

where k_v and k_r representing adjustable gain values, while the subscript d denotes references to a predetermined ideal profiles. Implicit guidance laws generate commands based on references (in this case, ideal position, velocity, and acceleration descent profiles) as opposed to explicit guidance laws which enforce targeting conditions.

If $\mathbf{a}_d$ is assumed to be a quadratic function of time, and hence $\mathbf{v}_d$ to be cubic, setting $k_v = 6$ and $k_r = 12$, equation 3.4 returns the APDG law (equation 3.3) (Lu, 2018). A^{2}PDG maintains the aforementioned constraints on the acceleration and velocity profiles and combines the gain values (k_v and k_r) into one tunable parameter, k_r. The result is the following guidance law (Lu, 2018):

$$\mathbf{a}(t) = \frac{2}{t_{go}}\left(1 - \frac{1}{3}k_r\right)[\mathbf{v}_f - \mathbf{v}(t)] + \frac{k_r}{t_{go}^2}[\mathbf{x}_f - \mathbf{x}(t) - \mathbf{v}(t)t_{go}] + \frac{1}{6}(k_r - 6)\mathbf{a}_f + \frac{1}{6}(k_r - 12)\mathbf{g}. \tag{3.5}$$

Varying the gain parameter, k_r serves as a trade between trajectory shaping and propellant consumption. Notably, the limits of k_r are bounded by $6 \leq k_r \leq 12$. Setting $k_r = 6$, a_f cancels from the equation 3.5 and therefore reduces to E-guidance. If $k_r = 12$, $\mathbf{g}$ is removed from equation 3.5 and thus the original APDG law is recovered.

D'Souza (1997) shows that a guidance law that is a linear function of the initial and final states including a non-linear time to-go variable, specifically:

$$a = -4\frac{\mathbf{v}(t) - \mathbf{v}_f}{t_{go}} - 6\frac{\mathbf{x}(t) - \mathbf{x}_f}{t_{go}^2} - \mathbf{g} \tag{3.6}$$

is optimal with respect to the performance index:

$$J = \Gamma t_f + \frac{1}{2}\int_{t_0}^{t_f} \|\mathbf{a_T}\|^2 dt \tag{3.7}$$

where Γ is a weighted final time parameter. Note that D'Souza's guidance law (equation 3.6) is a special case of equation 3.4 with $k_v = 4$ and $k_r = 6$, and thus lies within the adjustable family of guidance laws described by A^{2}PDG. However, it is important to recognize that the performance index (equation 3.7) does not represent strict fuel minimization that would be described by the performance index:

$$J = \int_{t_0}^{t_f} \|\mathbf{a_T}\| dt \tag{3.8}$$

Thus, the tune-ability of A^{2}PDG does not necessarily represent a direct trade between trajectory shaping and fuel optimization, but rather the optimality of a closely related problem.

Chapter 4

The Second-Order Cone Programming (SOCP) Based Guidance Method

Thus far, the guidance methods presented divided the three-dimensional soft-landing problem into three separate component systems of equations; the SOCP method adopts a different approach. The SOCP guidance method as proposed by Akmee et al. (2013), includes constraints limiting the vehicle to a region above the target landing site defined by a glide slope (in order to avoid trajectories near or along the surface), and an upper velocity limit. The constraints on the control input (commanded thrust) limit the magnitude to be between extrema:

$$0 \leq \|\mathbf{T_{min}}\| \leq \|\mathbf{T}(\mathbf{t})\| \leq \|\mathbf{T_{max}}\|. \tag{4.1}$$

A thrust pointing constraint is also included:

$$\hat{\mathbf{n}}^T \frac{\mathbf{T_c}(t)}{\|\mathbf{T_c}(\mathbf{t})\|} \geq cos(\theta). \tag{4.2}$$

In equation 4.2, $\hat{\mathbf{n}}^T$ represents a unitary pointing direction vector, while θ representing the maximum allowable deviation of the controlled thrust vector from this direction. Since the method models the vehicle as a point mass, this constraint is included in the place of explicit attitude limits. The separation of translation and attitude control is reasonable to assume since attitude correction maneuvers can be executed within a time scale significantly smaller than translations.

The SOCP method is implemented in two phases. First, leaving the remaining time of flight unconstrained, the landing distance error in minimized by solving the following problem (Akmee et al., 2013):

$$\min_{t_f, \mathbf{T}_C} \|\mathbf{x}(t_f) - \mathbf{q}\| \tag{4.3}$$

subject to:

$$\dot{\mathbf{x}}(t) = A(\omega)\mathbf{x}(t) + B\left(\mathbf{g} + \frac{\mathbf{T}_c(t)}{m}\right); \qquad \dot{m}(t) = -\alpha\|\mathbf{T}_c(t)\| \tag{4.4}$$

$$\mathbf{x}(t) \in \mathbf{X} \tag{4.5}$$

and the typical soft-landing boundary constraints: $\mathbf{e}_1^T\mathbf{x}(t_f) = 0$ and $\dot{\mathbf{x}}(t_f) = 0$ in addition to equations 4.1 and equation 4.2. In equation 4.3, $\mathbf{q}$ represents the targeted landing point, while A and B in equation 4.4 represent matrices that account for the effects of the planet's rotation on

the dynamics of the system. The fuel consumption rate is represented by α. Equation 4.5 is the glide slope constraint previously mentioned, bounding $\mathbf{x}(t)$ within the region X. It is important to recognize that multiple solution trajectories could exist such that they all reach the same landing error. The next step would be to minimizes the fuel consumption to select the optimal trajectory, however, the lower bound on the magnitude of the control thrust in equation 4.1 is a non-convex constraints.

Non-convex constraints pose an issue to global optimization problems. They have the potential to split a problem into multiple feasible regions and enable local optimal solutions within the parameter search space. Determining if a non-convex optimization problem is feasible and that a solution is globally optimal can be computationally taxing. Akmee et al. (2013) present an ingenious method of transforming the minimum thrust constraint from non-convex to convex by relaxing the problem through the introduction a new parameter, Γ(t) that functions similar to an upper limit on the magnitude of the thrust. To complete the convexification of the entire problem, a relaxed form of the landing error constraint is adopted during the fuel optimization step. The reframed problem follows (Akmee et al., 2013):

$$\min_{t_f, \mathbf{T}_C, \Gamma} \|\mathbf{x}(t_f) - \mathbf{q}\| \tag{4.6}$$

subject to:

$$\dot{\mathbf{x}}(t) = A(\omega)\mathbf{x}(t) + B\left(\mathbf{g} + \frac{\mathbf{T}_c(t)}{m}\right); \qquad \dot{m}(t) = -\alpha\Gamma(t) \tag{4.7}$$

$$\|\mathbf{T}_c\| \leq \Gamma(t); \qquad 0 \leq \|\mathbf{T_{min}}\| \leq \Gamma(t) \leq \|\mathbf{T_{max}}\| \tag{4.8}$$

$$\hat{\mathbf{n}}^T \mathbf{T_c}(t) \geq \Gamma(t) cos(\theta) \tag{4.9}$$

and equation 4.5 in addition to the typical soft-landing boundary constraints mentioned previously. Continuing, the fuel optimization step involves (Akmee et al., 2013):

$$\min_{t_f, \mathbf{T}_C, \Gamma} \int_{t_0}^{t_f} \Gamma(t) dt \tag{4.10}$$

subject to equations 4.7, 4.8, 4.9, and:

$$\|\mathbf{x}(t_f) - \mathbf{q}\| \leq \|\mathbf{d}_{min} - \mathbf{q}\| \tag{4.11}$$

where $\mathbf{d}_{min}$ represents the minimum landing distance error calculated in the previous step. Note that equation 4.11 represents a relaxation of the terminal landing location which is necessary to keep the problem convex. Even with this modification, the solution will remain optimal with regards to landing error because the minimal reachable landing error lies on the boundary of the space described by equation 4.11, that otherwise contains unreachable landing locations.

The landing error and fuel optimization steps can be discretized, and in addition to a change of variables, both be posed as second-order cone programming (SOCP) problems (Acikmese and Ploen, 2007). SOCP problems are more broadly studied within optimization research and are well known to be efficiently solved via interior point methods (IPMs). IPMs converge within a tolerance of the optimum solution within a finite, known number of iterations

(Steinfeldt et al., 2008). IPMs also converge with polynomial time complexity (which is a measure of how long an algorithm will take to execute as a function of the size of the input), thus giving the SOCP method an advantage over alternative iterative optimization methods.

Ultimately, the SOCP guidance technique generates landing error and fuel optimized feasible trajectories, observing the most physically representative constraints of any guidance method mentioned thus far, while guaranteeing convergence to said optimal solution in a finite, predictable time. Only made possible by recent developments, the SOCP method has yet to be applied to a planetary exploration mission descent, but shows promising potential.

Chapter 5

A Comparison of Guidance Algorithms

Figure 5.1 represents a complete block diagram of a general guidance control system.

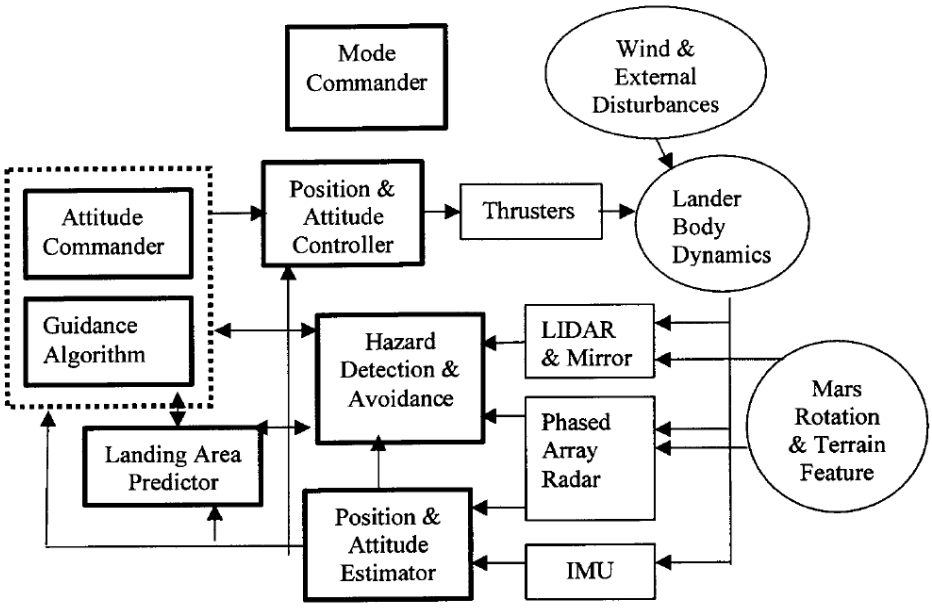

Figure 5.1: Schematic of a guidance control system (Wong et al., 2002)

For a given vehicle and mission, this diagram would be identical for different guidance methods with the exception of how the steps within the dotted boundary, “Guidance Algorithm” and “Attitude Commander” are defined. Focusing on the guidance algorithm, the following block diagrams represent a further detailed breakdown of each guidance method studied in this paper.

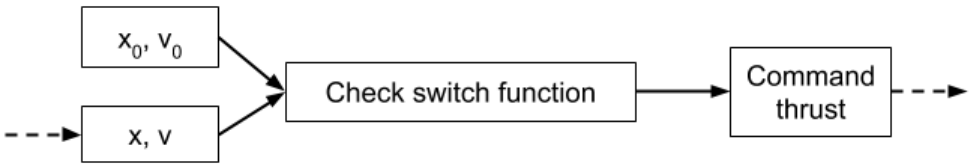

Figure 5.2: Meditch Block schematic

Figure 5.2, The Meditch switching method is purely dependent on recognizing when condition are met to initiate a full thrust burn. Perhaps the simplest form of powered descent guidance, the Meditch switching method has the benefit of proven fuel optimally in one dimension. However, this technique does not accommodate trajectory shaping.

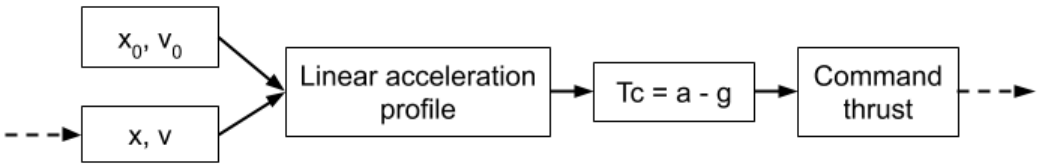

Figure 5.3: APDG Block schematic

The APDG method (Figure 5.3) incorporates trajectory shaping into its guidance algorithm, which while not fuel optimal, minimizes a performance metric closely related to fuel consumption. The APDG as developed is a explicit guidance method based around an assumption of a quadratic acceleration profile. APDG is noteworthy for its simplicity, but at the cost of control saturation (commanding thrust beyond the capabilities of the vehicle).

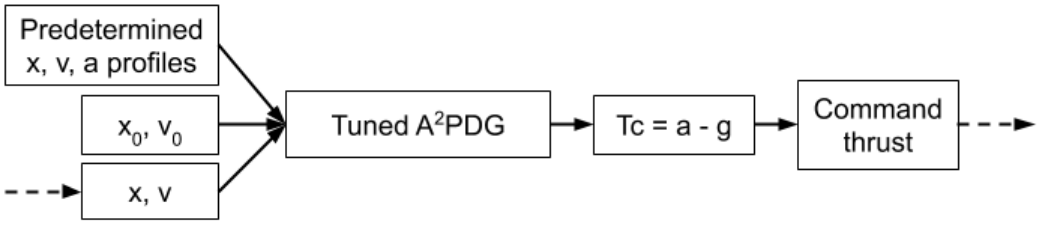

Figure 5.4: A^{2}PDG Block schematic

A^{2}PDG builds upon APDG transforming, into a tunable implicit guidance algorithm described by 5.4. Within the A^{2}PDG frame work, mission designers are provided the freedom to trade between propellant consumption and trajectory shaping, however the trajectory is based on a predetermined profile.

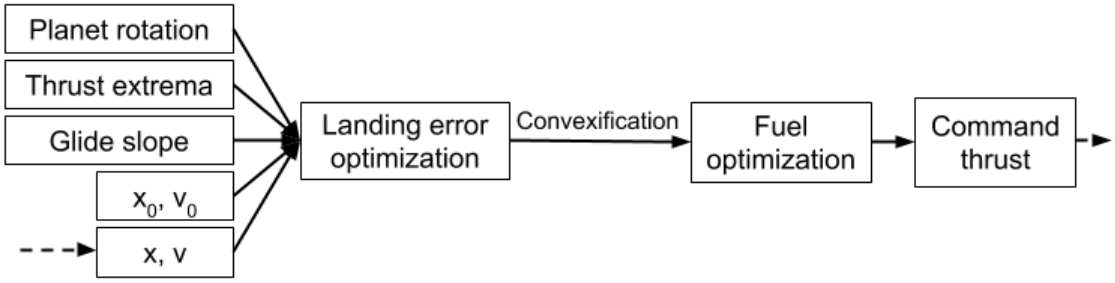

Figure 5.5: SOCP Block schematic

The SOCP method (Figure 5.5) as presented is the most complete guidance algorithm of all. The SOCP method accounts for the minimum thrust control constraint and planet rotation, while generating guaranteed achievable control profiles in a finite, predictable number of iterations. SOCP also includes methods to adapt the trajectory if the pinpoint target is unreachable. SOCP minimizes the landing distance error and then generates a fuel optimized trajectory to reach a landing point at that distance.

While A^2PDG and others like it offer computation simplicity and heritage, SOCP offers the most complete approach to solving the powered descent guidance problem, performance benefits and added robustness.

Chapter 6

Conclusion

A^{2}PDG offers the heritage of the flight proven APDG technique in the form of a repackaged, tunable implicit guidance law. The iterative, explicit SOCP method, while more computationally intensive than A^{2}PDG, offers significant performance gains while accounting for the most representative constraints of the techniques studied. However, the adoption of the A^{2}PDG method does not necessarily lead to a more simplistic guidance algorithm compared to a SOCP equivalent system. Techniques such as A^{2}PDG often require additional guidance routines such as powered descent initiation.

The SOCP guidance method, while not flight proven within the context of a planetary exploration mission, show great potential regarding optimality, robustness, and feasibility. The work of Akmee et al. (2013) has significantly improved the practicality of incorporating such a method into future missions.

In a direct comparison, A^{2}PDG offers heritage in place of SOCP's superior modern

optimization approach. A^2PDG has the advantage of computational simplicity in comparison to the iterative process of IPM incorporated into the SOCP method. While computation resources may have limited space exploration missions of the past, the modern power of on-board guidance computers is extremely capable.

In the immediate future at the time this paper was written, the *Mars 2020* rover will represent the next demonstration of powered descent guidance. Suprisingly, the powered descent phase of the Mars Science Laboratory architecture (on which the *Curiosity* and *Mars 2020* rovers are based) does not claim any fuel optimality, but rather

> "...the emphasis instead was on ease of analysis and, hence, ease of Validation and Verification of the system performance in the presence of altitude estimate errors due to terrain relief" (Dwyer Cianciolo, 2017).

Through a widespread understanding of optimization guidance methods and refinement of the analysis techniques used to study them, fuel optimization can become a primary focus of powered descent system design. This is critically important as the evolving demands of space exploration missions require evermore refined and robust EDL capabilities.

Bibliography

Acikmese, B. and Ploen, S. R. (2007). Convex Programming Approach to Powered Descent Guidance for Mars Landing. *Journal of Guidance, Control, and Dynamics*, Vol. 30(No. 5): pp.1353–1366. doi:10.2514/1.27553.

Akmee, B., Carson, J. M., and Blackmore, L. (2013). Lossless convexification of non-convex control bound and pointing constraints of the soft landing optimal control problem. *IEEE Transactions on Control Systems Technology*, Vol. 21(No. 6): pp. 2104–2113 doi:10.1109/TCST.2012.2237346.

Bennett, F. V. (1970). Apollo lunar descent and ascent trajectories. Technical Report No. NASA-TM-X-58040, March 1970.

Brand, T., Fuhrman, L., Geller, D., Hattis, P., Paschall, S., and Tao, Y. (2004). GN&C Technology Needed to Achieve Pinpoint Landing Accuracy at Mars. In *AIAA/AAS Astrodynamics Specialist Conference and Exhibit*, Guidance, Navigation, and Control and Co-located Conferences. American Institute of Aeronautics and Astronautics. doi:10.2514/6.2004-4748.

Braun, R. D. and Manning, R. M. (2007). Mars Exploration Entry, Descent, and Landing Challenges. *Journal of Spacecraft and Rockets*, Vol. 44(No. 2): pp.310–323 doi: 10.2514/1.25116.

D'Souza, C. (1997). An optimal guidance law for planetary landing. In *Guidance, Navigation, and Control Conference*, Guidance, Navigation, and Control and Co-located Conferences. American Institute of Aeronautics and Astronautics. doi:10.2514/6.1997-3709.

Dwyer Cianciolo, A. (2017). Entry, Descent, and Landing Guidance and Control Approaches to Satisfy Mars Human Mission Landing Criteria. In *27th AAS/AIAA Space Flight Mechanics Meeting*, San Antonio, TX, United States.

Klumpp, A. R. (1974). Apollo Lunar Descent Guidance. *Automatica*, Vol. 10(No. 2): pp.133–146. doi: 10.1016/0005–1098(74)90019–3.

Lu, P. (2018). Augmented Apollo Powered Descent Guidance. *Journal of Guidance, Control, and Dynamics*, Vol. 42(No. 3): pp.447–457. doi: 10.2514/1.G004048.

Meditch, J. (1964). On the problem of optimal thrust programming for a lunar soft landing. *IEEE Transactions on Automatic Control*, Vol. 9(No. 4): pp.477–484 doi:10.1109/TAC.1964.1105758.

Steinfeldt, B., Grant, M., Matz, D., Braun, R., and Barton, G. (2008). Guidance, Navigation, and Control Technology System Trades for Mars Pinpoint Landing. In *AIAA Atmospheric Flight Mechanics Conference and Exhibit*, Honolulu, Hawaii. American Institute of Aeronautics and Astronautics doi:10.2514/6.2008-6216.

Wong, E. C., Singht, G., and Masciarellif, J. P. (2002). Autonomous Guidance and Control Design for Hazard Avoidance and. In *Safe Landing on Mars, AIAA Paper 2002-4502, Atmospheric Flight Mechanics Conference*.